Bioactive Materials 6 (2021) 3085–3096

Contents lists available at ScienceDirect

Bioactive Materials

journal homepage: www.sciencedirect.com/journal/bioactive-materials

An in situ-forming polyzwitterion hydrogel: Towards vitreous substitute application

Binbin He [a], Jianhai Yang [a,**], Yang Liu [a], Xianhua Xie [a], Huijie Hao [b], Xiaoli Xing [b,***], Wenguang Liu [a,*]

[a] School of Materials Science and Engineering, Tianjin Key Laboratory of Composite and Functional Materials, Tianjin University, Tianjin, 300350, China
[b] Tianjin International Joint Research and Development Centre of Ophthalmology and Vision Science, Eye Institute and School of Optometry, Tianjin Medical University Eye Hospital, Tianjin, 300384, China

ARTICLE INFO

Keywords:
Zwitterion
Hydrogel
Anti-fouling
Vitreous substitute

ABSTRACT

Development of a biostable and biosafe vitreous substitute is highly desirable, but remains a grand challenge. Herein, we propose a novel strategy for constructing a readily administered vitreous substitute based on a thiol-acrylate clickable polyzwitterion macromonomer. A biocompatible multivinyl polycarboxybetaine (PCB-OAA) macromonomer is designed and synthesized, and mixed with dithiothreitol (DTT) via a Michael addition reaction to form a hydrogel in vitreous cavity. This resultant PCB-OAA hydrogel exhibits controllable gelation time, super anti-fouling ability against proteins and cells, excellent biocompatibility, and approximate key parameters to human vitreous body including equilibrium water content, density, optical properties, modulus. Remarkably, outperforming clinically used silicone oil in biocompatibility, this rapidly formed hydrogel in the vitreous cavity of rabbit eyes remains stable in vitreous cavity, showing an appealing ability to prevent significantly inflammatory response, fibrosis and complications such as raised intraocular pressure (IOP), and cataract formation. This zwitterionic polymer hydrogel holds great potential as a vitreous substitute.

1. Introduction

Vitreous body is a hyaloid and gelatinous substance filling the vitreous cavity between the lens and retina. It is essentially a highly hydrated avascular extracellular gel matrix primarily composed of collagen, hyaluronic acid and 98–99 wt% water [1,2]. The vitreous cannot only maintain normal orbit turgor to position the retina, act as a shock absorber dampening the intraocular motions and vibrations, but also keep the light path clear and ensure the circulation of nutrient and metabolites [2]. However, vitreous abnormality including liquefaction, hemorrhage and infection can result in dysfunction and other ocular diseases such as retinal detachment, cataract and glaucoma. Ocular trauma and various ocular diseases with aging (e.g. hemorrhage, proliferative diabetic retinopathy, retinal detachment) may cause blindness; thus total removal and replacement of the vitreous is clinically required in these cases [3]. Currently, perfluorocarbon (PFC) liquids are used as a temporary substitute, while gas and silicone oil is frequently used for medium- and long-term substitutes, respectively. However, their potential toxicity and *in vivo* instability have limited their long-term clinical applications [4,5]. For instance, emulsification of silicone oil can cause unexpected complications such as retinal toxicity, nerve damage, increased intraocular pressure (IOP), temporary loss of vision, and cataract formation [6,7].

An ideal vitreous substitute should satisfy the following criteria: (i) biocompatibility with neighboring tissues, (ii) high transparency, (iii) appropriate modulus to act as a tamponade to keep the retina in place, (iv) *in vivo* long-term stability, (v) injectable and extractable ability through a small gauge needle, (vi) serving as the intraocular tamponade for retinal detachment surgery [8]. Recently, several in situ crosslinked polymer hydrogels with high water contents and transparency have been explored as vitreous substitutes, such as hyaluronic acid (HA) [9,10], silk [11], polyethylene glycol (PEG) [12,13], or polyacrylamide

Peer review under responsibility of KeAi Communications Co., Ltd.
* Corresponding author.
** Corresponding author.
*** Corresponding author.
E-mail addresses: jianhaiyang@tju.edu.cn (J. Yang), xxlteh@126.com (X. Xing), wgliu@tju.edu.cn (W. Liu).

https://doi.org/10.1016/j.bioactmat.2021.02.029
Received 28 December 2020; Received in revised form 6 February 2021; Accepted 20 February 2021
Available online 9 March 2021

(PAM) [14] and its copolymer hydrogels [15]. These crosslinkings are mostly based on thiol oxidation, thiol-acrylate Michael addition reaction, and enzymatic oxidation. However, most of these polymers tend to be degraded or elicit foreign body reaction post-implantation, ruling out the possibility of developing long-term vitreous substitutes. As a hydrophilic and biocompatible polymer, PEG has been extensively investigated as bioinert and antifouling biomaterials for the purpose of reducing immunogenicity. Nevertheless, its *in vivo* degradation and potential anti-PEG immune responses may reduce physiological retention times of bioconstructs [16,17]. Therefore, there is a significant clinical need to develop a biostable and bioinert hydrogel-based vitreous substitute with a very simple in situ gelling ability and key features resembling natural vitreous body.

Zwitterionic polymers have drawn significant attention as stealth biomaterials because of their outstanding anti-fouling capabilities against proteins and cells [18–20]. An ultra-low-fouling zwitterionic poly(carboxybetaine methacrylate) hydrogel has been shown to significantly reduce the inflammatory response and the formation of collagen capsule surrounding it in mice's subcutaneous tissue [21]. To suppress intraocular biofouling, an in situ-forming sulfobetaine-based zwitterionic copolymer hydrogel was recently developed as a vitreous substitute, and encouraging outcomes were achieved [22]. However, long-term implanation was not reported.

Among the polybetaines including carboxybetaine (CB), sulfobetaine (SB), and phosphorylcholine, CB-based polyzwitterion is a unique biomimetic material since its structure is similar to glycine betaine that is taken in on the daily basis by human [18]. Previous studies revealed that CB polyzwitterion could resist protein adsorption more effectively than SB polyzwitterion due to its moderate self-association property [23]. Lately, our group reported on a supramolecular polymer hydrogel by copolymerization of hydrogen bonding monomer N-acryloyl glycinamide (NAGA) and carboxybetaine monomer (CBAA) [24]. The resultant hydrogel exhibited a shear-thinning property and could be injected into the vitreous cavity to serve as a stable vitreous substitute without eliciting complications due to the introduction of antifouling poly(carboxybetaine). Nonetheless, this shear-thinning hydrogel needed to be strictly screened from many formulations of highly swollen and swelling stable hydrogels.

To develop a biostable and biosafe vitreous substitute, we proposed a simple and clinically operable approach to prepare polycarboxybetaine hydrogel by in situ Michael addition reaction between multivinyl polycarboxybetaine macromonomer (MPM) and thiol. The MPM, poly-2-((2-hydroxy-3-(methacryloyloxy)propyl) dimethyl ammonio) acetate carrying acrylate groups (PCB-OAA) was first synthesized, and its higher molecular weight would not cause damage to tissue due to a lower diffusion rate into the cells [25]. The MPM would react with dithiothreitol (DTT), a biocompatible reductant frequently used in biological systems [26,27], to form a highly hydrated hydrogel in rabbit's vitreous cavity (Fig. 1). We anticipated that injection of PCB-OAA with DTT into the rabbit's eye would contribute to a rapid gelation, and multiple crosslinks combined with monosulfide bonds formed would ensure the stability of hydrogel in the vitreous cavity. This polycarboxybetaine-based hydrogel remained stable in vitreous cavity without eliciting immunological response.

2. Materials and methods

2.1. Materials

4,4′-Azobis (4-cyanovaleric acid) (ACVA, 98%), hydroxyethyl methacrylate (HEMA, 97%), DL-dithiothreitol (DTT, 98%), N,N′-bis (acryloyl)cystamine (BAC, 98%), 2-hydroxy-2-methyl-1-phenyl-1-propanone (IRGACURE-1173, 98%), 3-(4,5-dimethyl-2-thiazolyl)-2,5-diphenyl-2-H-tetrazolium bromide (MTT, 98%) were purchased from Sigma-Aldrich (Shanghai, China). Acrylic anhydride (AA, 97%) was obtained from Shaoyuan Chemical Technology Co., Ltd (Shanghai,

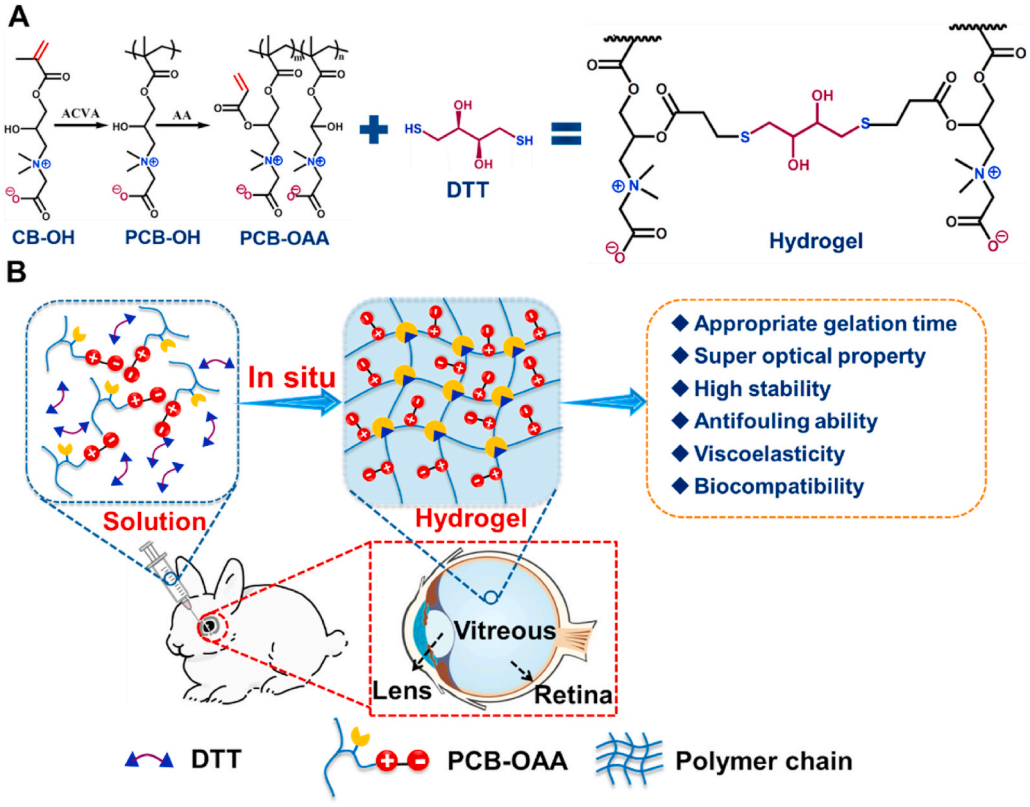

Fig. 1. (A) Synthesis procedure, molecular structures of PCB-OAA zwitterionic polymer and PCB-OAA-DTT hydrogel. (B) Schematic illustration of injection of PCB-OAA and DTT into rabbit vitreous cavity to form a hydrogel in situ, serving as a vitreous substitute.

China). Silicone oil (SO, Oxane 5700) was obtained from Bauschlomb Company. Ellman reagent 5,5′-dithiobis-(2-nitrobenzoic acid) (DTNB, 98%) was purchased from Innochem Technology Co., Ltd (Beijing, China). Mouse fibroblast cells (L929) and human retinal epithelium cells (ARPE-19) were obtained from Procell Technology Co., Ltd (Wuhan, China). 2-((2-hydroxy-3-(methacryloyloxy)propyl) dimethyl ammonio) acetate (CB–OH) was synthesized according to the previously published method [28]. All other chemicals and solvent were analytical reagents and used as received.

2.2. Synthesis of zwitterionic polymer PCB-OAA

Zwitterionic polymer PCB-OAA was synthesized by a one-pot procedure. Briefly, zwitterionic monomer CB-OH (4.90 g, 20 mmol) was dissolved in 80 mL ultrapure water, and ACVA (0.028 g, 0.1 mmol) was added to the solution and stirred for 30 min until complete dissolution. The mixture was purged with nitrogen several times to ensure the oxygen-free environment, and then stirred at 70 °C for about 16 h, to obtain a PCB-OH polymer solution. After that, the solution was cooled down to room temperature, followed by addition of $NaHCO_3$ (8.4 g, 0.1 mol) and 20 mL ultrapure water. Then the acrylic anhydride (10 mL, 87 mmol) was added dropwise and stirred at 25 °C for 24 h. The resultant solution was dialyzed in ultrapure water for 3 days, and lyophilized to obtain the zwitterionic polymer PCB-OAA. The degree of substitution (DS) for acrylate groups in polymer PCB-OAA was calculated from ^{1}H NMR spectra.

2.3. Preparation of PCB-OAA hydrogels

An appropriate mass of PCB-OAA polymer was dissolved in phosphate-buffered saline (PBS, pH 7.4) to form a homogeneous solution with various concentrations. A 200 mM DTT solution was prepared by dissolving DTT in PBS. Then PCB-OAA solutions were mixed with DTT solution to prepare PCB-OAA-x hydrogel, where x represented the initial concentration of PCB-OAA polymer. The volume ratio of PCB-OAA solution to DTT solution was fixed at 10/1 throughout the study.

2.4. Characterizations

The structure of polymer was characterized by a nuclear magnetic resonance (NMR) spectrometer (AVANCE III, 400 MHz, Bruker) using D_2O as the solvent. The molecular weight of the polymer was determined by gel permeation chromatography (GPC, DAWN HELEOS, WYATT). The concentration of the polymer aqueous solution was set at 5.0 mg/mL, and 0.1 mol/L $NaNO_3$ was used as the mobile phase with a flow rate of 1.0 mL/min. The gelation time was determined at 37 °C by using the vial-inversion method, and recorded as the time when the sample could support its own weight. The refractive indexes of hydrogels were assessed on an Abbe refractometer (WYA-2W, Lumsail Industrial) using water as a blank sample. The equilibrium water contents (EWCs) of the hydrogels were measured using a gravimetric method [29]. The light transmittance of hydrogel was determined using a UV/vis spectrophotometer (GENESYS 180, Thermo Fisher) over a wavelength range from 380 to 780 nm using PBS as a blank sample.

2.5. Swelling behavior of hydrogels

The swelling behavior of the hydrogel was determined *in vitro* by incubating the hydrogels in physiological saline solution (0.9 wt% NaCl) at 37 °C for up to 1 month. The fresh PCB-OAA hydrogels were weighed ($m_{t=0}$), and then immersed in the aforementioned solution and weighed (m_t) at different time points. The swelling ratio was defined as $m_t/m_{t=0}$. This test was conducted in triplicate and the average values were calculated.

2.6. Conversion rate of thiol and acrylate groups

The Ellman method was utilized to determine the conversion rate of thiol group [30]. In brief, the hydrogel samples (20 μL) were placed into a 5 mL DTNB solution (0.08 mg/mL in PBS). After incubation for 10 min at room temperature, the absorbance of the supernatant at different times was measured by UV/vis spectrophotometer at a wavelength of 412 nm. DTT was used as the standard sample to prepare the calibration curve for thiol quantification.

The conversion rate of acrylate groups in PCB-OAA hydrogels was determined by ^{1}H NMR spectra. Briefly, after forming hydrogels in NMR tubes using D_2O as solvent, the samples were placed in room temperature for 2 days to ensure complete reaction, followed by ^{1}H NMR characterization. The conversion rate (CR) of acrylate groups was calculated by comparing the degree of substitution of acrylate groups.

2.7. Measurement of nonspecific protein adsorption

Evaluation of the nonspecific protein adsorption was carried out according to previously reported method [31]. Cylindrical hydrogels were immersed in 1 mL bovine serum albumin solution (BSA, 2 mg/mL) and incubated at 37 °C for 90 min. The hydrogels were taken out carefully and washed out with PBS to remove loosely adsorbed proteins. The adsorbed proteins were detached by ultrasound for 10 min, and measured by a micro-BCA protein assay kit (Boster Biotechnology Co., Ltd) according to the standard protocol. The test was conducted in triplicate and average values were recorded.

2.8. Cell attachment and cytotoxicity assay

Cell attachment test was conducted by incubating cells on the hydrogel surfaces. 200 μL PCB-OAA solution and 20 μL DTT solution were added into a 48-well plate and incubated for 24 h at 37 °C to ensure the complete gelation. Mouse fibroblast (L929) cells were then seeded on the surface of hydrogels at a density of 2×10^4 cells/well. After incubation for 24 h under the atmosphere of 5% CO_2 at 37 °C, the surface of each hydrogel as well as the tissue culture polystyrene surface (TCPS, control) were gently rinsed with the media, and images before and after rinsing were photographed on a microscope (CKX41, Olympus). Then, L929 cells was incubated for another 24 and 48 h, and photographed again.

MTT assay was used to investigate the cytocompatibility of PCB-OAA hydrogels, PCB-OAA and DTT solutions. Initially, the PCB-OAA solution and DTT solution were separately prepared and filtered by 0.22 μm membrane for sterilization, and then the solutions were diluted to different concentrations (20–100 mg/mL for PCB-OAA solutions, and 25–200 mM for DTT solutions). ARPE-19 cells were seeded into 96-well plates with a density of 1×10^4 cells/well, and incubated for 24 h in 200 μL complete dulbecco's modified eagle medium/nutrient mixture F-12 (DMEM/F12, supplemented with 10% fetal bovine serum (FBS) and 1% penicillin-streptomycin) under the atmosphere of 5% CO_2 at 37 °C. The medium was replaced with 200 μL complete DMEM/F12 containing 20 μL PCB-OAA hydrogels or PCB-OAA and DTT solutions. After co-incubation for 24, 48 and 72 h, the medium was discarded and replaced with 180 μL fresh medium and 20 μL MTT solution (5 mg/mL). After incubation for another 4 h, the medium was replaced with 200 μL dimethyl sulfoxide (DMSO). The absorbance was recorded at 570 nm using a microplate reader (Infinite M200 PRO, Tecan, Switzerland), and the relative cell viability (%) was calculated with the reported protocol [24].

2.9. Rheological measurements

The rheological behavior of hydrogels was investigated using a rheometer (MCR302, Anton Paar) with a temperature-controlled Peltier plate system. Firstly, a thin layer of hydrogel was formed and a 25 mm

cone plate was lowered onto the hydrogel sample with a working gap of 0.049 mm. During the measurement, silicone oil was placed around the plate to prevent water evaporation. Oscillation strain sweep from 0.1 to 100% at a frequency of 1 Hz was performed to determine the linear viscoelastic region. Time-sweep oscillatory test was carried out at 1 Hz frequency and 1% strain for up to 1800 s after mixing PCB-OAA and DTT solution. Frequency sweep from 0.01 to 10 Hz was performed with 1% strain, and the storage modulus (G') and loss modulus (G'') were monitored. Shear creep analysis was conducted by applying 0.5 or 1.0 Pa constant shear stress to the hydrogels under both nominal creep and a creep recovery time of 150 s, respectively. Then the shear creep compliance and strain were recorded. All tests were performed at 37 °C to simulate the physiological condition *in vivo*.

2.10. Subcutaneous implantation

Six weeks old C57BL/6 male mice weighing ≈20 g were used for subcutaneous implantation of hydrogels. Before implantation, 7% PCB-OAA solution and DTT (200 mM) solution were respectively filtered by 0.22 μm membrane for sterilization, and transferred into a 1 mL sterile syringe equipped with a 22 G needle. Then, 50 μL of above-mentioned mixture solution was subcutaneously injected into two separate sites on the mice's dorsum. After 14 and 28 days postimplantation, the mice were euthanatized. Sample and surrounding tissues were collected and fixed in 4% paraformaldehyde, embedded in paraffin. The sections were stained with hematoxylin and eosin (H&E) or Masson's trichrome (M&T), and scanned by Panoramic scanner (P250 FLASH, 3DHISTECH) for further histological analysis.

2.11. Vitreous substitution surgery

All the protocols for the animal experiments were carried out in accordance with the guidelines of the Council for the Purpose of Control and Supervision of Experiments on Animals, Government of China. The animal experiments were approved by the Animal Ethics Committee of Nankai Hospital, China. Intravitreal injection and postoperative examinations. Fifteen adult male rabbits (weighing about 2.5 kg) were randomly divided into three groups (five rabbits per group): sham-operated group (served for evaluation of the effect of operation itself), silicone oil group (Oxane 5700), and PCB-OAA hydrogel group. Considering the individual difference among all rabbits, all surgeries were performed on the right eyes of rabbits (surgical), and the left eyes were the nonsurgical eyes, serving as a normal control (normal). Before the experiments, all rabbits had been inspected so that no original ophthalmic complication or abnormality was found; 7% PCB-OAA solution and DTT (200 mM) solution were respectively filtered by 0.22 μm membrane for sterilization. Rabbits were firstly anesthetized with xylazine hydrochloride (0.5–0.6 mL) through intramuscular injection into thighs of rabbits, and then original vitreous body (0.3–0.4 mL) was extracted and replaced with the same volume of silicone oil or PCB-OAA hydrogel, respectively. Incisions were placed 3.5 mm posterior to the limbus and were made vertical to the limbus at an angle of 45° to the sclera, and then PCB-OAA hydrogel precursor was injected into the vitreous cavity with a 22 G needle after vitrectomy surgery. For sham-operated group, the vitreous of the right eye was extracted and injected immediately back to the cavity. After surgery, tobramycin eye ointment (Alcon, U.S.A) was used to reduce postoperative inflammation, and the rabbits were housed in individual cages and kept under controlled temperature and humidity with free access to food and water. During all the surgery, the extraction and injection were slow avoiding of collapse of the eyes.

2.12. Ocular examination

Intraocular pressure (IOP) was measured through the center of the cornea by using a full auto tonometer (TX-F, Canon) before surgery and at predetermined times post-operation. B-ultrasound examination was performed using an ultrasonic diagnostic instrument (MD2300s, MEDA Co., Ltd, Tianjin, China). Fundus photography was performed using a digital retinal camera (CR-2, Canon) and fluorescein angiography was assessed by a digital angiography (HRA SPECTRALIS, Heidelberg Engineering), with the animals under general anesthesia. For fluorescein angiography, 0.2 mL sodium fluorescein was injected into the auricular vein of the rabbits.

Retinal function was assessed by electroretinogram (ERG). Briefly, the pupils were dilated with 5% tropicamide and animals were anesthetized. Then, the animals were dark-adapted for 20 min. The ERG setup was consisted of a contact lens electrode for each eye, and reference needle electrodes were positioned at the bilateral temple and the top of the head. Standard ERGs were recorded by the Espion Visual Electrophysiology System from Diagnosis, LLC (Littleton, MA, USA). Subsequently, the animals were light-adapted for 10 min and ERGs were also recorded. The individual components of an ERG examination were named according to the adaptive state of the eye (dark-adapted (DA); light-adapted (LA)) and the stimulus strength in candela-second per square meter. Herein, DA 0.01 reflected the use of a 0.01 cd × s/m^2 flash delivered under dark adaptation, and LA 3 reflected the use of a 2.562 cd × s/m^2 flash delivered under photopic conditions.

B-ultrasound examination, fundus photography, fluorescein angiography, and ERG tests were performed at 1 month and 6 months post-operation. Ocular examinations mentioned above were performed by one ophthalmologist blinded to experimental treatment.

2.13. Histology assessment

At 6 months post-surgery, the rabbits were euthanized, and the operated and normal eyeballs were collected, fixed with 4% formaldehyde, embedded in paraffin. The sections were stained with hematoxylin and eosin (H&E) and scanned by Panoramic scanner (P250 FLASH, 3DHISTECH) for further histological analysis.

2.14. Statistical analysis

Data are expressed as the mean ± standard deviation (SD). Statistical analysis was performed using two population student's t-test to evaluate the protein adsorption, b-wave in ERG tests and intraocular pressure examination. Statistical significance is denoted by $p^* < 0.05$, $p^{***} < 0.001$.

3. Results and discussion

3.1. Preparation and characterizations of PCB-OAA hydrogels

In order to construct an injectable antifouling hydrogel for vitreous substitute, we first synthesized a zwitterionic monomer 2-((2-hydroxy-3-(methacryloyloxy)propyl) dimethylammonio) acetate (CB–OH) by opening ring reaction of glycidyl methacrylate with sarcosine according to the previous report [28]. Next, the CB-OH was polymerized to form PCB-OH containing hydroxyl groups in side chains. Then PCB-OH reacted with acrylic anhydride in a weak alkaline solution to form a multivinyl acrylate groups-tethered polycarboxybetaine macromonomer (MPM, final yielding is 83.7%). As shown in the ^{1}H NMR spectra of PCB-OH and PCB-OAA, new peaks appearing at 6.0–6.6 ppm were attributable to the acrylate group, confirming the desired chemical structure (Fig. S1). Based on the integral area ratio of peak H_{8+9+10} (4H) to peak H_6 (6H), the degree of substitution for acrylate groups was estimated to be 18.75%. In addition, the molecular weight of PCB-OAA was determined to be 3.1×10^5 Da (PDI = 1.5) by using GPC (Fig. S2).

The thiol-acrylate Michael addition reaction is known as a highly efficient and catalyst-free reaction under physiological conditions [32]. Next, the MPM obtained was mixed with DTT to examine the gelling behavior. We found that the gelation occurred at a minimal

concentration of 7% PCB-OAA under a physiological pH when the initial concentration of DTT was 200 mM and the volume ratio of PCB-OAA to DTT was 10/1 (Fig. S3). Then we prepared a series of PCB-OAA hydrogels with different polymer concentrations, i.e. 7%, 8.5% and 10%, and the resultant hydrogels were named as PCB-OAA-7, PCB-OAA-8.5 and PCB-OAA-10, respectively. The final concentration of DTT was calculated to be 20 mM, and the acrylate/thiol molar ratios in the PCB-OAA-7, PCB-OAA-8.5, and PCB-OAA-10 hydrogel were 1.3, 1.6, 1.8, respectively (Table S1). We used the inverted vial method to preliminarily determine the gelation time of the PCB-OAA hydrogels. The gelation times of PCB-OAA-7, PCB-OAA-8.5, and PCB-OAA-10 hydrogel were about 3.2 min, 1.7 min and 1 min, respectively (Fig. 2A). This indicates that a higher concentration of PCB-OAA led to a shorter gelation time due to rapid contact of reactive acrylate groups with DTT. To investigate the activity of thiol-acrylate Michael addition reaction between PCB-OAA and DTT, the conversion rate of thiol and acrylate groups was calculated by using the Ellman method [30] and ^{1}H NMR spectra, respectively. Fig. S4 shows that the conversion rates of thiol groups in PCB-OAA-7, PCB-OAA-8.5 and PCB-OAA-10 hydrogel were 92.0%, 66.1%, and 64.8%, respectively, within 1 min, and thiols in the three gels all reached more than 98% conversion rates within 5 min (Table S1), indicating that the thiol groups were nearly completely consumed within 5 min and the remaining traces of DTT in the PCB-OAA hydrogel would not affect the biocompatibility of hydrogel. Furthermore, conversion rates of acrylate groups for PCB-OAA-7, PCB-OAA-8.5 and PCB-OAA-10 hydrogel were 80.0%, 62.7%, 60.0%, respectively (Fig. S5, Table S2). The theoretical crosslinking degrees of PCB-OAA-7, PCB-OAA-8.5 and PCB-OAA-10 hydrogels were calculated as 1769, 2176, 2450 g/mol, and the corresponding actual crosslinking degrees were 2211, 3470, 4083 g/mol (Table S2).

As a vitreous substitute, the appropriate expandible property of injectable hydrogel is critical for maintaining its function. High swelling after injection in vitreous cavity can induce the severe increase of IOP and glaucoma [33]. While non-swelling hydrogel can not resist the swelling counter-force of natural vitreous body to keep retina in place, which may cause retinal detachment [34]. Therefore, the expandible behavior of PCB-OAA hydrogel immersed in physiological saline solution (0.9 wt% NaCl) simulating physiological condition *in vivo* was measured. The swelling profiles of the PCB-OAA hydrogels are shown in Fig. 2B. It is seen that the hydrogels immersed in physiological saline solution reached swelling equilibrium within 3 days, and obvious change of mass was not observed in the following one month. The final swelling ratios were determined to be about 1.6, 2.3, and 3.0 for PCB-OAA-7, PCB-OAA-8.5, and PCB-OAA-10 hydrogel, respectively. As expected, the swelling ratio value was increased at a higher PCB-OAA content due to the decrease in cross-linking density with DTT. This result indicates that the PCB-OAA hydrogels possessed not only an adjustable polymer concentration-dependent swelling behavior, but also a good swelling stability. Here, the swelling ratio value of PCB-OAA-7 hydrogel was close to that of previously reported vitreous substitutes

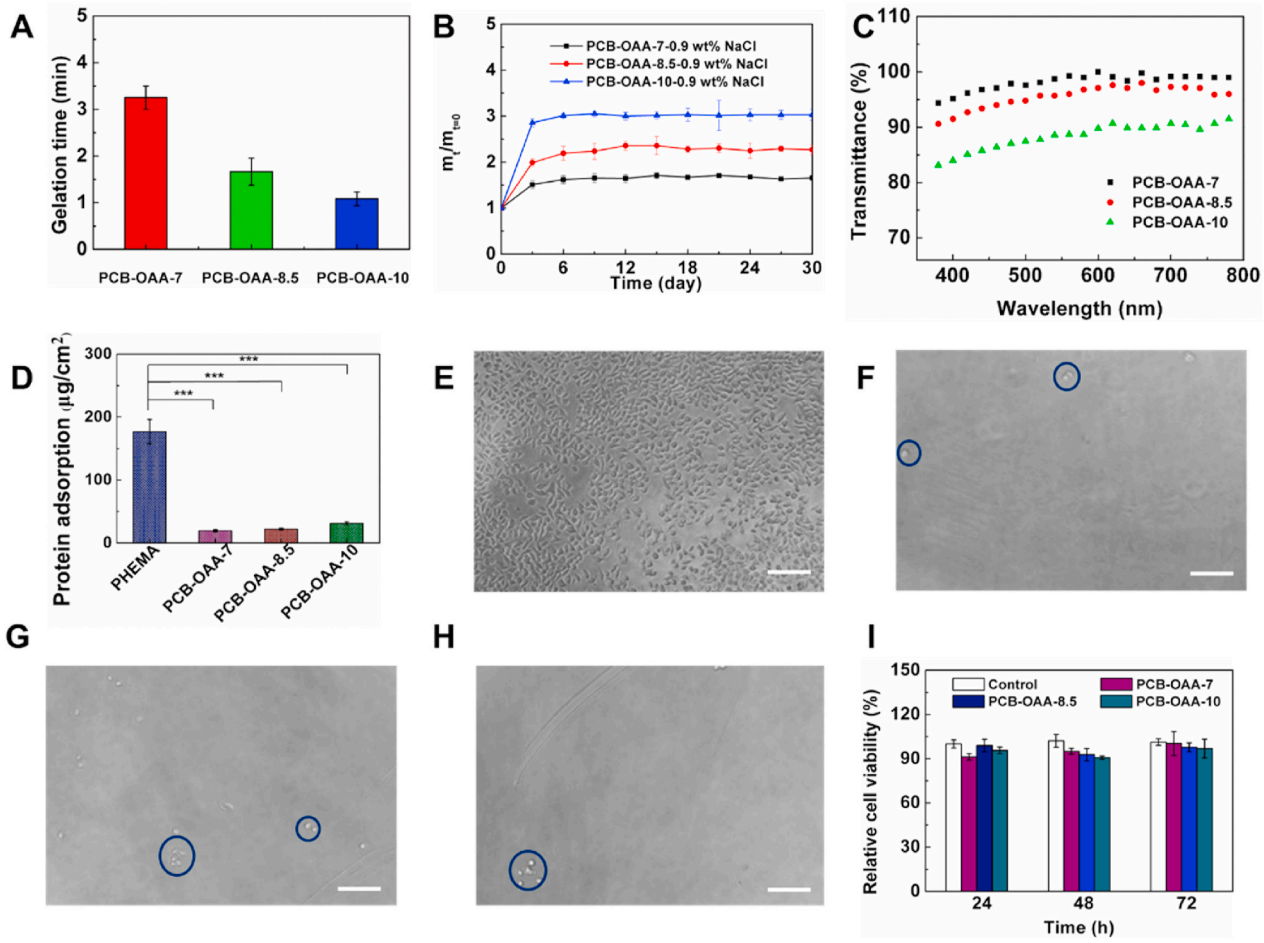

Fig. 2. Characterizations of PCB-OAA hydrogels. (A) Gelation time of PCB-OAA hydrogels by vial-inversion test at 37 °C. (B) Swelling ratios of PCB-OAA hydrogels in physiological saline solution (0.9 wt% NaCl) at 37 °C for 1 month. (C) Light transmittance of the hydrogels over a wavelength range of 380–780 nm. (D) Protein adsorption of PHEMA hydrogel (control) and PCB-OAA hydrogels. (***$p < 0.001$). (E–H) Images of cellular attachment on tissue culture polystyrene surface (TCPS), PCB-OAA-7, PCB-OAA-8.5, and PCB-OAA-10 hydrogel after rinsing, respectively. The remaining cells were denoted by blue circles. The scale bars were 200 μm. (I) Relative cell viability of ARPE-19 cells co-cultured with PCB-OAA hydrogels for 24, 48 and 72 h.

[22,35], suggesting the expandible property of PCB-OAA-7 hydrogel makes it suitable as a vitreous substitute.

We next evaluated the optical properties of the hydrogels including light transmittance and refractive index that are the key factors to realize the light transmission in the eye and maintain normal vision [36,37]. Fig. 2C displays the light transmittance of hydrogels at the wavelength range from 380 to 780 nm. Both the PCB-OAA-7 and PCB-OAA-8.5 hydrogels exhibited over 90% light transmittance, whereas less than 90% transmittance was obtained for PCB-OAA-10 hydrogel. It is noted that all the hydrogels exhibited lower light transmittance at a lower wavelength below 450 nm, which was in accordance with the ideal behavior of native vitreous (~85% transmittance at 400 nm) [1,2]. In contrast, silicone oil can allow for 100% light transmittance at 400 nm [9]. This feature is beneficial for impeding ultraviolet harm to retinal epithelium [38]. The light transmittance values of PCB-OAA-7 and PCB-OAA-8.5 and PCB-OAA-10 hydrogel at a wavelength of 550 nm were 98.5%, 96.5% and 88.6%, respectively. Increasing polymer concentration contributed to the attenuation of light transmittance through the hydrogel since somewhat heterogeneous gelation occurred after mixing concentrated PCB-OAA with DTT. All the PCB-OAA hydrogel exhibited about a 1.34 refractive index (RI) that is only slightly higher than that of human vitreous body. The vitreous of human adults has been identified to have a >90% light transmittance, a RI of 1.3345–1.3348, a density of 1.0053–1.0089, and >98 wt% water content [1]. In comparison, the light transmittance, RI, density and water content of the PCB-OAA-7 hydrogel were very close to those of human vitreous body (Table S3).

3.2. Antifouling capacity and cytotoxicity of the hydrogels

Nonspecific protein adsorption on the implant surfaces is considered to be the first and critical event in triggering a foreign body reaction and the formation of collagenous capsule [21,39]. To determine whether the PCB-OAA hydrogel demonstrated an antifouling capability, we first evaluated its protein-resistance performance. As depicted in Fig. 2D, the poly(hydroxyethyl methacrylate) (PHEMA) hydrogel that is usually considered as a low biofouling material exhibited 176.8 μg/cm^2 protein adsorption. Comparatively, the amount of adsorbed protein on all the PCB-OAA hydrogels significantly decreased to below 50 μg/cm^2. The PCB-OAA-7, PCB-OAA-8.5, and PCB-OAA-10 hydrogel exhibited protein adsoption of 19.4, 22.2 and 31.4 μg/cm^2, respectively. Clearly, the PCB-OAA-7 hydrogel was the highest resistant to nonspecific protein adsorption, and the resistance was slightly weakened with the increase of PCB-OAA concentrations. This is probably because the excess acrylate groups in the PCB-OAA-10 hydrogel network may undergo Michael addition reaction with the amino groups in proteins, thus resulting in more adsorbed proteins on the surface. We next investigated the cell attachment on the PCB-OAA hydrogel. After 24 h incubation, TCPS supported substantial L929 cellular adhesion, and almost all cells were flattened with a spread morphology and protrusions before rinsing. However, cells seeded on the surface of PCB-OAA hydrogels aggregated and maintained a rounded morphology, which was the specific behavior of unattached cells (Fig. S6). As shown in Fig. 2E–H and Fig. S6, after gently rinsing, the cells on TCPS tightly adhered to the surface and normal cell proliferation was observed in the following 24 and 48 h incubation, whereas almost all the cells were detached from hydrogels and only very few rounded cells were maintained on the surface of hydrogels after 24 and 48 h incubation. These results indicate that the PCB-OAA hydrogel possessed an excellent antifouling capacity.

To inspect the cytocompatibility of PCB-OAA hydrogel, we first evaluated the effect of PCB-OAA and DTT concentrations on the viability of human retinal epithelium cells (ARPE-19) after co-cultured for 24, 48 and 72 h. Considering the residual contents of acrylate group and thiol group in the hydrogel, the maximum concentrations of PCB-OAA and DTT incubated with cells were set at 10 mg/mL and 20 mM, respectively. We found that PCB-OAA solutions with various concentrations all exhibited above 90% cell survival rate throughout 72 h of co-incubation (Fig. S7A). Although the relative cell viability of DTT solutions declined over time, the final cell survival rates of all concentrations were above 75% (Fig. S7B). Indeed, the initial DTT in precursor solution was 20 mM, and could be consumed near to 98% within 5 min, Therefore, the DTT could no longer cause long-term cytotoxicity. Fig. 2I displayed that all the PCB-OAA hydrogels exhibited above 90% survival rate even after co-incubating for 72 h, suggesting that the PCB-OAA hydrogel had better cytocompatibility and the very few remaining DTT in hydrogel would not cause cytotoxicity, which further proves that the above mentioned antifouling abilities of the hydrogels were irrelevant to their cytotoxicity.

To further inspect the biocompatibility and anti-fibrosis ability of hydrogels *in vivo*, the PCB-OAA-7 hydrogel was subcutaneously injected into the C57BL/6 mice. As depicted in Fig. S8, there are negligible inflammatory cells or deposited collagen around the tissue throughout 28 days of observation. The excellent biocompatibility and antifouing ability portends promising potential as artificial transplant.

3.3. Rheological behavior of the PCB-OAA hydrogels

To evaluate whether the PCB-OAA hydrogel has the similar viscoelasticity with that of natural vitreous body so that it can maintain a shock-absorbing function [40], the rheological behaviors of the hydrogels were investigated in our experiment. We firstly determined the linear viscoelasticity region of the hydrogels by oscillatory strain sweep test, and then selected a strain of 1% for the following test. Fig. 3A displays the change in G' and G'' of as-prepared hydrogels as a function of time. The gelation time of PCB-OAA-7 hydrogel calculated from the crossover point of G' and G'' is 300 s, but the crossover points of PCB-OAA-8.5 and PCB-OAA-10 hydrogels could not be detected due to their fast gelation behavior. As presented in the figure, all the PCB-OAA hydrogels exhibited an enhanced value of G' with increasing time immediately after mixing, indicating the growing number of cross-linking points in hydrogel network. By contrast, the PCB-OAA-7 hydrogel underwent the slowest increasing trend, but the G' value was finally close to that of PCB-OAA-8.5 hydrogel and higher than that of PCB-OAA-10 hydrogel (Table S4), suggesting that the least cross-linking points were formed in the PCB-OAA-10 hydrogel network. It is accepted that the G' of hydrogel is critical for withstanding the saccadic movement of eye, which can vary from a small amplitude with a frequency of 10°/s to a large amplitude with a frequency of 300°/s [41]. Thus, the effect of frequency on the G' value of PCB-OAA hydrogels was studied by frequency sweep mode (Fig. 3B). One can see that the G' values for all the PCB-OAA hydrogels are always dominant over the G'' and remained constant value at the whole frequency range (0.01–10 Hz). And the G' values were determined to be 233.1 Pa, 233.2 Pa and 111.3 Pa for PCB-OAA-7, PCB-OAA-8.5, and PCB-OAA-10 hydrogel, respectively (Table S4), hinting that these hydrogels had a stable rheological property at a high frequency. To inspect the stability of PCB-OAA hydrogel after swelling, we performed the frequency sweep test to record storage modulus change of PCB-OAA hydrogel immersed in physiological saline solution for 1 month (Fig. 3C). Clearly, all the G' values were almost constant, suggesting they maintained a stable hydrogel state even after immersing for 1 month. It is noted that all the G' values were lower than those of original hydrogels to a different extent. To be more detail, there was a 17.7%, 55.5% and 79.6% decline in storage modulus, that is, from original 233.1 Pa, 233.2 Pa, 111.3 Pa–191.8 Pa, 103.8, 22.7 Pa, respectively, for PCB-OAA-7, PCB-OAA-8.5, and PCB-OAA-10 hydrogel (Fig. 3D), It is not difficult to understand that further swelling after long-term immersion in saline solution led to the decrease of mechanical properties. While a higher crosslinking density could better restrain water from diffusing into the gel network.

To further understand the relationship between the network structure and G', we calculated the average mesh size (ξ, distance between the entanglement points) and the average molecular weight between cross-

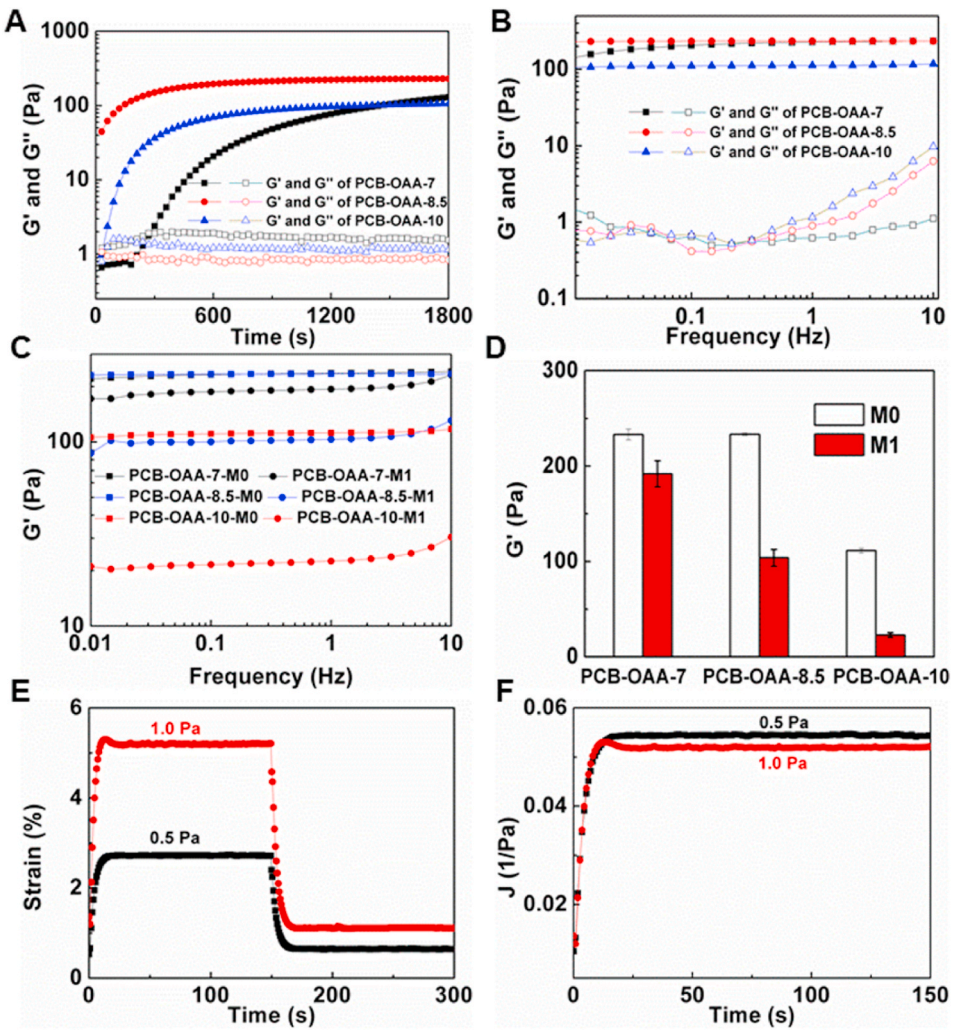

Fig. 3. Rheological properties of PCB-OAA hydrogels. (A) Time sweep curves of PCB-OAA hydrogels at 1 Hz frequency and 1% strain within 1800 s. (B) Frequency sweep curves of PCB-OAA hydrogels at a frequency range from 0.01 to 10 Hz at 1% strain. Storage modulus (G') and loss modulus (G'') were recorded. (C) Frequency sweep curves of PCB-OAA hydrogels before (M0) and after (M1) immersion for 1 month in physiological saline solution. (D) Average values of G' for PCB-OAA hydrogels before and after immersion. (E) Strain curves and (F) creep compliance curves of PCB-OAA-7 hydrogel plotted as a function of time in shear creep test under different applied shear stress (0.5 and 1.0 Pa). All tests were performed for at least 3 times at 37 °C.

links in the rheological test by using the following equations, which are applicable to hydrogels with an elastic character [42,43].

$$\xi = \left(\frac{G' N_A}{RT}\right)^{-\frac{1}{3}} \quad (1)$$

$$Mc = \frac{cRT}{G'} \quad (2)$$

where N_A is the Avogadro constant (6.02×10^{23}/mol), T is absolute temperature, R is the molar gas constant (8.314 J/(mol × K)), c is the polymer concentration (kg/m^3), Mc is the average molecular weight between cross-links, and G' is the averaged storage modulus in frequency sweep test. Rheological and related structural parameters are listed in Table S4. It can be found that both PCB-OAA-7 and PCB-OAA-8.5 hydrogel had the same ξ value (26.4 nm) and approximate Mc value (770, and 940 g/mol, respectively), while PCB-OAA-10 hydrogel had the highest value of ξ (33.8 nm) and Mc (2320 g/mol), suggesting a densely cross-linked network for both PCB-OAA-7 and PCB-OAA-8.5 hydrogel, and loosely cross-linked network for PCB-OAA-10 hydrogel, which is in line with the above-mentioned crosslinking degree analysis. These results indicate that increasing polymer concentration would weaken the density of cross-linking since the amount of DTT was constant.

It was previously reported that the value of G' for bovine vitreous body with intact membrane was 120 Pa [44]. A filling biomaterial with higher mechanical integrity will better absorb shock, provide effective tamponade and increase stability and residence time (preferably over 3 months) [1,2]. Taking into account various factors including appropriate gelation time, swelling ratio, storage modulus, optical properties, superior antifouling capacity and swelling stability, the PCB-OAA-7 hydrogel with a 233.1 Pa storage modulus that was close to the previously reported vitreous substitutes [11,22,45], was chosen for further study.

Viscoelasticity is an intrinsic property of vitreous humor and a crucial factor for any hydrogel-based vitreous substitute since this nature helps to protect the eye from external mechanical impact. The viscous behavior of vitreous substitute can make it act as a shock-absorber through its own volumetric shrinkage, while the elasticity affords the rapid volume recovery of vitreous without altering eye shape [46]. We next performed the shear creep analysis of PCB-OAA-7 hydrogel to determine the change in both strain and creep compliance under different shear stresses. As illustrated in Fig. 3E, when the stress was unloaded, the PCB-OAA-7 hydrogel underwent a partial recovery, including instantaneous recovery and retarded recovery until the steady state was reached. The first region corresponded to the elastic response of the hydrogel to a sudden change of shear stress, and the second region reflected a viscous effect. It is worth noting that the strain did not decline in a linear pattern as a function of time (representative pattern for liquid); the steady state was finally achieved, and the strain was not zero. All the above results verify the viscoelasticity of PCB-OAA-7 hydrogels. Furthermore, the similar change trend in shear creep compliance was also observed (Fig. 3F), and the value of the shear creep compliance (~0.05) in different applied stress (0.5 and 1.0 Pa) was in

the range of the normal value (0.02–1 Pa) of native vitreous body [46], further illustrating the similar rheological property of the PCB-OAA-7 hydrogel to native vitreous body.

3.4. In vivo evaluation of the hydrogel as an vitreous substitute

The outstanding comprehensive properties of PCB-OAA-7 hydrogel encouraged us to explore it as a vitreous substitute. *In vivo* evaluation was performed by injecting a mixture of PCB-OAA (7 wt%) solution and DTT (200 mM) solution into the vitreous cavity of rabbits to achieve in-situ forming hydrogel. The clinically used silicone oil (SO, Oxane 5700) served as a control group to highlight the therapeutic effect of PCB-OAA-7 hydrogel as an excellent vitreous substitute, and sham-operated group was used to examine the influence of the operation itself. Since the rabbit vitreous adheres to the retina tightly, it is unlikely to remove it completely. The rabbit has a higher ratio of lens to vitreous-chamber volume (1.27) than that of humans (0.25), which may result in a low accessibility and the inadvertent trauma to the lens during standard vitrectomy [47]. Therefore, only a partial vitrectomy was performed to avoid touching the lens and causing the consequent cataract and retinal detachment according to the previous reports [15,47]. Taking into account the individual differences among rabbits, an operation was performed on right eyes, and left eyes were left as normal control. Video S1–S3 show the vitreous substitution process of sham, SO and PCB-OAA hydrogel groups *in vivo*. During the whole surgery for SO and PCB-OAA hydrogel groups, original vitreous body was extracted out and replaced with the same volume of silicone oil or PCB-OAA hydrogel, respectively. Incisions were placed 3.5 mm posterior to the limbus, and collapse or shrinkage of eyeball was not observed in the surgery.

Supplementary video related to this article can be found at https://doi.org/10.1016/j.bioactmat.2021.02.029

B-scan ultrasound examination was performed to evaluate retinal integrity at 1 month and 6 months post-surgery, respectively. As shown in Fig. 4A and B, the crescent shape represented the lens, and the posterior smooth arc signified the attached retina. No abnormal changes of high or medium echoes, and no complications (hemorrhage and retinal detachment) were observed in the normal group, sham group and PCB-OAA-7 hydrogel group at 1 month and 6 months post-surgery. Notably, some flocculent echoes were observed in the SO group, which might be abnormal echoes resulted from the difference in sound velocity between silicone oil and water [48].

To further inspect the therapeutic effect of the vitreous substitute,

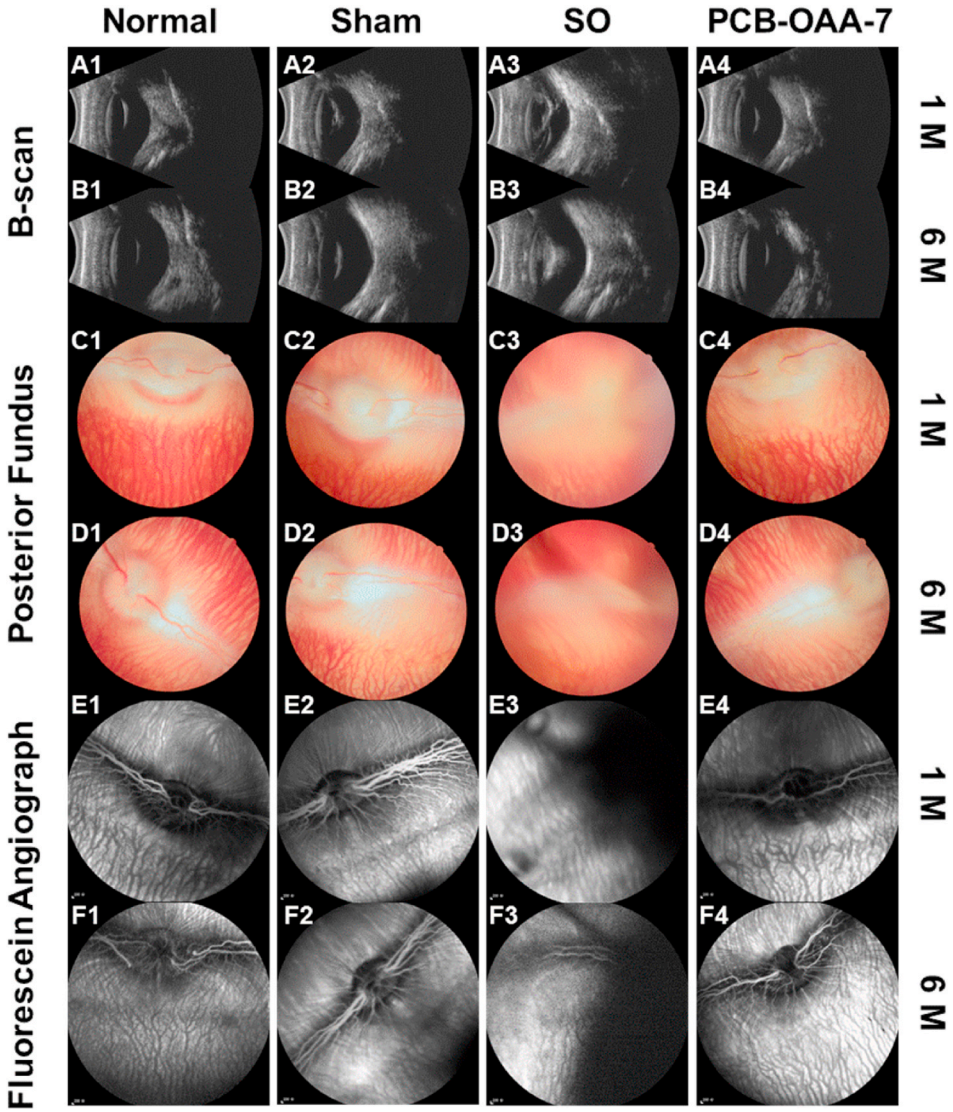

Fig. 4. In vivo images of rabbit eyes at 1 month (1 M) and 6 months (6 M) post-operation. (A–B) B-scan ultrasound images; (C–D) posterior fundus photographs; (E–F) fluorescein angiographs. Column (A1-F1): Normal eye groups, Column (A2-F2): Sham-operated groups. Column (A3-F3): Silicone oil (SO) groups. Column (A4-F4): PCB-OAA-7 hydrogel groups.

funduscopic examination and fluorescein angiography were conducted. As shown in Fig. 4C and D, for normal, sham, and PCB-OAA-7 hydrogel group, the funduscopic images at 1 month and 6 months post-surgery demonstrate that the dioptric media still remained fine transparency, and no vitreous opacity, vitreous hemorrhage, membrane formation, or chorioretinal lesions were observed in the rabbit eyes; the blood capillary and central blood vessels were clearly visible. Similarly, clear blood vessel could be viewed in the fluorescein angiography images of all the three groups via injecting fluorescein contrast agent (Fig. 4E and F). Furthermore, the optic discs in all the three groups were obvious and clear, suggesting that the light could smoothly travel throughout the entire eye. There was negligible difference in all the three groups, indicating that operation did not exert an adverse effect on the rabbit eye, and the PCB-OAA-7 hydrogel exhibited better functions in the vitreous cavity. While for the SO group, the funduscopic image and fluorescein angiograph image were both obscure (Fig. 4C3, D3 and 4E3, F3). This is probably because SO induced cataract, glaucoma or hemorrhage after operation due to the emulsification tendency of hydrophobic silicone oil when contacted with aqueous humor [6,7].

We next used electroretinography (ERG) to assess the response of the retina under scotopic (dark-adapted, DA) and photopic (light-adapted, LA) conditions. In principle, ERG a-wave and b-wave revealed the function of photoreceptor and müller cells, respectively. DA 0.01, DA 3, and LA 3 ERG respectively stood for rod response, the combined rod-cone maximal response, and the cone response, where 0.01 and 3 represented 0.01cd × s/m^2 and 2.562 cd × s/m^2 stimulus [49]. Partial waveforms of ERG tests are depicted in Fig. 5A and B (complete waveforms are shown in Fig. S9 and S10). Clearly, the surgical rabbit eyes in the sham, SO, and PCB-OAA-7 hydrogel group showed normal performance of scotopic, photopic and flicker ERGs that are similar to those of their corresponding normal eyes, indicating that there was no loss of inner retinal function at 1 month and 6 months. The b-wave amplitudes of DA 0.01, DA 3 and LA 3 ERGs for rabbit eyes in the sham, SO, and PCB-OAA-7 hydrogel groups at 1 month and 6 months were recorded in Fig. 5D–F and H-J, respectively. One can see that there was a slight increase in the b-wave amplitudes of the DA 0.01, DA 3 and LA 3 ERGs for surgical rabbit eyes in all the three surgical groups compared with their corresponding normal eyes at 1 month; while no significant change was observed at 6 month, demonstrating better photoreceptor functional activity, and substitution surgery itself and hydrogel implantation did not cause retinal dysfunction. Intraocular pressure (IOP) of rabbit eyes was also measured before and after operation at predetermined times. The IOP values within 2 weeks after surgery were within normal range, suggesting that the initial swelling of PCB-OAA hydrogel did not cause IOP abnormality at the early stage (Fig. S11). As shown in Fig. 5G and K, the IOP values of the surgical eyes in sham, SO, PCB-OAA-7 hydrogel groups at 1 month and 6 months did not show statistical difference with their corresponding eyes and all values were within the normal range that was similar to previous reports [50], indicating that partial vitrectomy would not cause IOP abnormality. All the above results indicate that the PCB-OAA-7 hydrogel could maintain the functions of the retina, and did not cause abnormal IOP after operation.

To further inspect the ocular state, external appearance and excised eyeball were displayed in Fig. 6A and B. No significant inflammation and any other abnormalities were observed in the sham and PCB-OAA-7 hydrogel group. These outcomes were similar to those of the normal eyes. While the SO group showed marked abnormality of opaque regions located in lens and vitreous body (Fig. 6A3, 6B3 and Fig. S12A2), implying a trend of cataract or vitreous opacity, which was resulted from the emulsification of SO. At 6 months post-surgery, the implanted PCB-OAA-7 hydrogel and silicone oil were removed from the vitreous cavity (Video S4), and the vitreous humor (VH) in each group exhibited both gel phase and liquid phase due to the normal age-related vitreous liquefaction (Fig. S12A1 and B). The VH in PCB-OAA-7 hydrogel group showed intact and highly transparent structure (Fig. S12A1), whereas the VH in SO group was emulsified and became opaque (Fig. S12A2). Interestingly, the gel phase of VH could be lifted by a tweezer, showing an appealing ability to bear its own weight. Even dragging on the surface

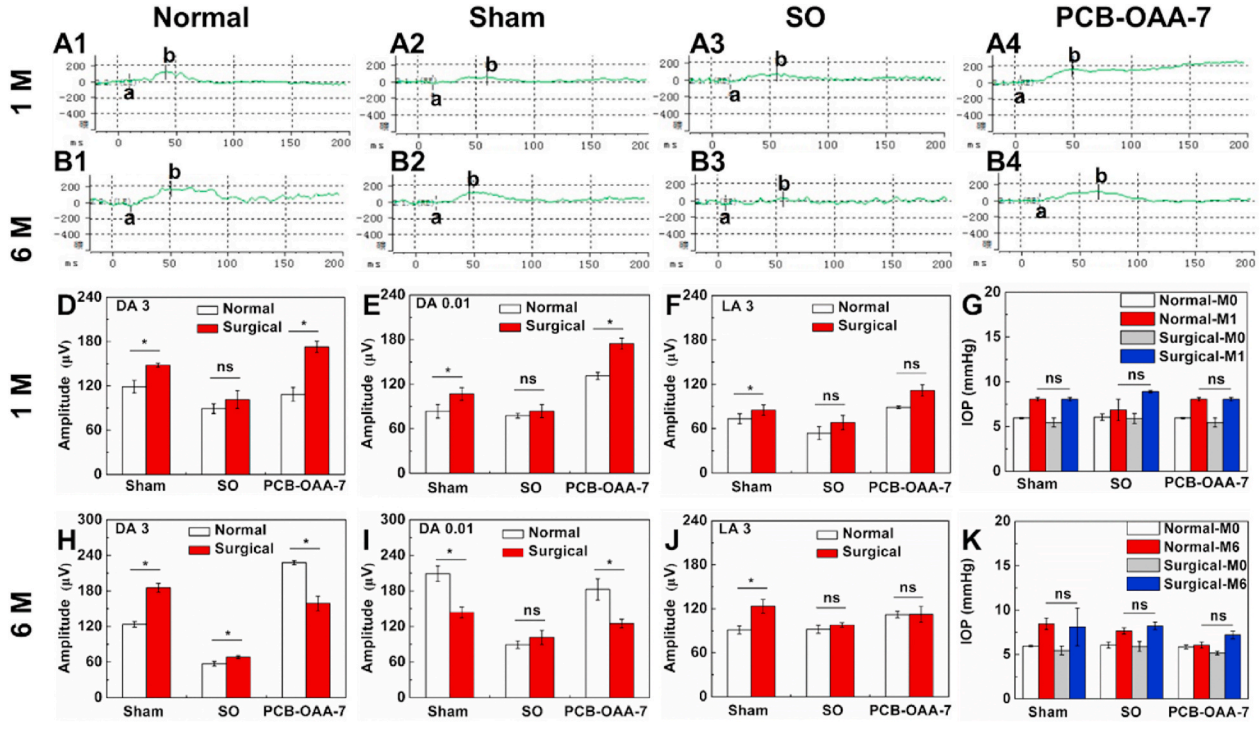

Fig. 5. The retina functions and intraocular pressure (IOP) of rabbit eyes at 1 month (1 M) or 6 months (6 M) post-operation. (A–B) Waveforms of dark-adapted 0.01 ERG (DA 0.01 ERG) tests for the normal, sham, SO and PCB-OAA-7 hydrogel group. (D-F, H-J) B-wave amplitudes recorded in dark-adapted 3 (DA 3), dark-adapted 0.01 (DA 0.01), light-adapted 3 (LA 3) ERG tests. (G and K) IOP values of rabbit eyes before (M0) and after (M1, M6) surgery at 1 month and 6 months, respectively (*P < 0.05, ns represents no statistical difference). The aforementioned 0.01 and 3 respectively represents 0.01 cd × s/m^2 and 2.562 cd × s/m^2 stimulus in ERG tests.

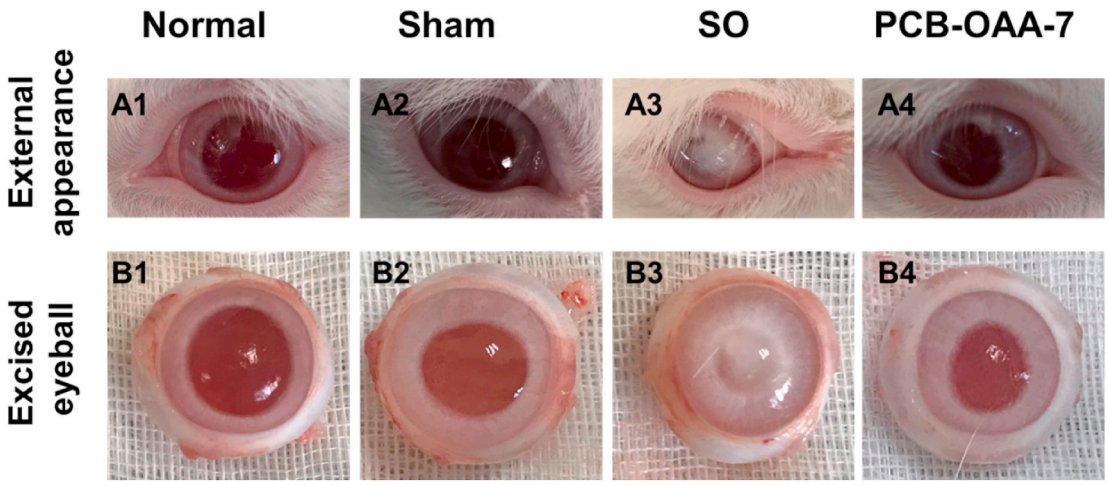

Fig. 6. Appearance of rabbit eyes at 6 months post-operation. (A) External appearance of rabbit eyes at 6 months post-operation. (B) Images of excised eyeball at 6 months post-operation. Obvious opaque region was shown in SO group while normal states were maintained in the other three groups.

of a bench could not deform it (Fig. S12C-E and Video S5–S6). This signifies the long-term stability of PCB-OAA-7 hydrogel in vitreous cavity. On the other hand, the better viscoelasticity the hydrogel maintained could aid in withstanding the deformation and motion of the eyeball, thus protecting the eye from both internal and external mechanical stress.

Supplementary video related to this article can be found at https://doi.org/10.1016/j.bioactmat.2021.02.029

Histopathological stainings were conducted at 6 months post-operation to examine variation of the eye tissues (Fig. 7). H&E staining shows that the normal structure of cornea, iris and retina was observed in the normal group, sham group and PCB-OAA-7 hydrogel group (Fig. 7A–C and Fig. S13). For the PCB-OAA-7 hydrogel group, there was no pathological inflammation response and fibrosis around retina, which was similar to the normal group and sham group (Fig. 7C4). While deformation and defective morphology of retina were present in the SO group, which was possibly resulted from SO infiltration (Fig. 7C3). Collectively, the in situ hydrogel formation method by Michael addition reaction between multivinyl polycarboxybetaine macromonomer with dithiol will provide a new possibility to construct a biocompatible vitreous substitute, whose functional evaluation as an intraocular tamponade for retinal detachment surgery will be preformed in the future work.

4. Conclusions

In summary, aiming at addressing the concerns often encountered in hydrogel designed to replace degenerated vitreous body in this work, we proposed a new strategy for constructing a readily administered biostable and biosafe vitreous substitute based on thiol-acrylate Michael addition reaction between acrylate modified polycarboxybetaine macromonomer and DTT. This polyzwitterionic hydrogel exhibited an appropriate gelation time, swelling ratio, storage modulus, approximate optical properties to human vitreous body, and a superior antifouling capacity and high stability. Co-injection of the polycarboxybetaine macromonomer and DTT precursor solutions contributed to rapid formation of a hydrogel in the rabbit eyes, perfectly filling the vitreous cavity, and keeping the retina in place. We demonstrated that this antifouling polyzwitterion hydrogel was superior to clinically used silicone oil in biocompatibility and remained table in the vitreous cavity without eliciting any adverse effects through the analyses of intraocular pressure (IOP) measurement, B-ultrasound examination, fundus

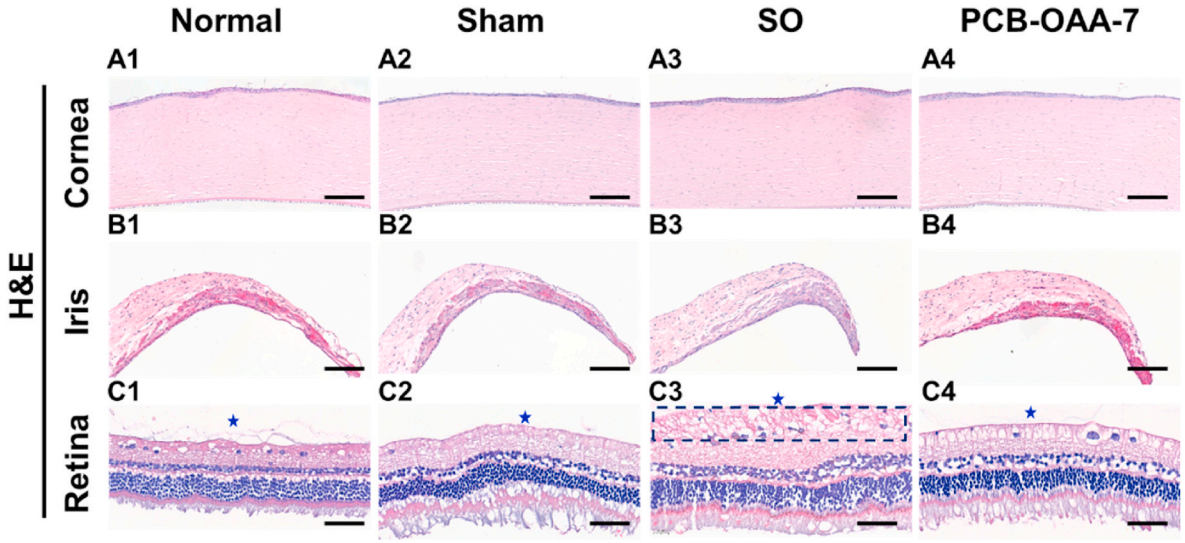

Fig. 7. Histopathological examinations and immunostaining of rabbit eyes at 6 months post-operation. (A–C) Hematoxylin and eosin (H&E) staining of cornea, iris, and retina, respectively. Blue asterisk and rectangle denotes the location of vitreous cavity in all groups and defective morphology in SO group, respectively. The scale bars of cornea and iris were 200 μm. The scale bar of retina was 40 μm.

photography, fluorescein angiography, electroretinogram as well as histopathological assay. We believe that this novel polyzwitterionic hydrogel represents a new option for artificial vitreous body.

CRediT authorship contribution statement

Binbin He: Investigation, Data curation, Methodology, Formal analysis, Writing – original draft. **Jianhai Yang:** Conceptualization, Data curation, Writing – original draft. **Yang Liu:** Investigation, Data curation. **Xianhua Xie:** Software, Data curation. **Huijie Hao:** Software, Data curation. **Xiaoli Xing:** Investigation, Data curation. **Wenguang Liu:** Conceptualization, Formal analysis, Writing – review & editing.

Declaration of competing interest

The authors declare that they have no known competing financial interests or personal relationships that could have appeared to influence the work reported in this paper.

Acknowledgments

We are thankful for the financial support of the National Natural Science Foundation (Grant Nos. 51733006, 52073203, 31771030).

Appendix A. Supplementary data

Supplementary data to this article can be found online at https://doi.org/10.1016/j.bioactmat.2021.02.029.

References

[1] T.T. Kleinberg, R.T. Tzekov, L. Stein, N. Ravi, S. Kaushal, Vitreous substitutes: a comprehensive review, Surv. Ophthalmol. 56 (4) (2011) 300–323.
[2] F. Baino, Towards an ideal biomaterial for vitreous replacement: historical overview and future trends, Acta Biomater. 7 (3) (2011) 921–935.
[3] F.M. Recchia, A.J. Ruby, C.A. Carvalho Recchia, Pars plana vitrectomy with removal of the internal limiting membrane in the treatment of persistent diabetic macular edema, Am. J. Ophthalmol. 139 (3) (2005) 447–454.
[4] C. Alovisi, C. Panico, U.D. Sanctis, C.M. Eandi, Vitreous substitutes: old and new materials in vitreoretinal surgery, J. Ophthalmol. 2017 (2017) 1–6.
[5] R. Kim, C. Baumal, Anterior segment complications related to vitreous substitutes, Ophthalmol. Clin. North. Am. 17 (4) (2004) 569–576.
[6] G.G. Giordano, M.F. Refojo, Silicone oils as vitreous substitutes, Prog. Polym. Sci. 23 (3) (1998) 509–532.
[7] A. Russo, F. Morescalchi, S. Donati, E. Gambicorti, C. Azzolini, C. Costagliola, F. Semeraro, Heavy and standard silicone oil: intraocular inflammation, Int. Ophthalmol. 38 (2) (2018) 855–867.
[8] M.J. Colthurst, R.L. Williams, P.S. Hiscott, I. Grierson, Biomaterials used in the posterior segment of the eye, Biomaterials 21 (7) (2000) 649–665.
[9] S. Suri, R. Banerjee, In vitro evaluation of in situ gels as short term vitreous substitutes, J. Biomed. Mater. Res. 79 (3) (2006) 650–664.
[10] H. Kim, H. Jeong, S. Han, S. Beack, B.W. Hwang, M. Shin, S.S. Oh, S.K. Hahn, Hyaluronate and its derivatives for customized biomedical applications, Biomaterials 123 (2017) 155–171.
[11] N.R. Raia, D. Jia, C.E. Ghezzi, M. Muthukumar, D.L. Kaplan, Characterization of silk-hyaluronic acid composite hydrogels towards vitreous humor substitutes, Biomaterials 233 (2020) 119729.
[12] K. Hayashi, F. Okamoto, S. Hoshi, T. Katashima, D.C. Zujur, X. Li, M. Shibayama, E. P. Gilbert, U. Chung, S. Ohba, T. Oshika, T. Sakai, Fast-forming hydrogel with ultralow polymeric content as an artificial vitreous body, Nat. Biomed. Eng. 1 (3) (2017) 44.
[13] Y. Tao, X. Tong, Y. Zhang, J. Lai, Y. Huang, Y. Jiang, B. Guo, Evaluation of an in situ chemically crosslinked hydrogel as a long-term vitreous substitute material, Acta Biomater. 9 (2) (2013) 5022–5030.
[14] K.E. Swindle-Reilly, M. Shah, P.D. Hamilton, T.A. Eskin, S. Kaushal, N. Ravi, Rabbit study of an in situ forming hydrogel vitreous substitute, Invest. Ophthalmol. Vis. Sci. 50 (10) (2009) 4840.
[15] S. Santhanam, J. Liang, J. Struckhoff, P.D. Hamilton, N. Ravi, Biomimetic hydrogel with tunable mechanical properties for vitreous substitutes, Acta Biomater. 43 (2016) 327–337.
[16] A.D. Lynn, T.R. Kyriakides, S.J. Bryant, Characterization of the in vitro macrophage response and in vivo host response to poly(ethylene glycol)-based hydrogels, J. Biomed. Mater. Res. 93 (3) (2010) 941–953.
[17] F. Zhang, M.W. King, Biodegradable polymers as the pivotal player in the design of tissue engineering scaffolds, Adv. Healthc. Mater. (2020) 1901358.
[18] S. Jiang, Z. Cao, Ultralow-louling, functionalizable, and hydrolyzable zwitterionic materials and their derivatives for biological applications, Adv. Mater. 22 (9) (2010) 920–932.
[19] L. Mi, S. Jiang, Synchronizing nonfouling and antimicrobial properties in a zwitterionic hydrogel, Biomaterials 33 (35) (2012) 8928–8933.
[20] T. Bai, S. Liu, F. Sun, A. Sinclair, L. Zhang, Q. Shao, S. Jiang, Zwitterionic fusion in hydrogels and spontaneous and time-independent self-healing under physiological conditions, Biomaterials 35 (13) (2014) 3926–3933.
[21] L. Zhang, Z. Cao, T. Bai, L. Carr, J. Ella-Menye, C. Irvin, B.D. Ratner, S. Jiang, Zwitterionic hydrogels implanted in mice resist the foreign-body reaction, Nat. Biotechnol. 31 (6) (2013) 553.
[22] J. Chang, Y. Tao, B. Wang, B. Guo, H. Xu, Y. Jiang, Y. Huang, An in situ-forming zwitterionic hydrogel as vitreous substitute, J. Mater. Chem. B 3 (6) (2015) 1097–1105.
[23] Y. Zhang, Y. Liu, B. Ren, D. Zhang, S. Xie, Y. Chang, J. Yang, J. Wu, L. Xu, J. Zheng, Fundamentals and applications of zwitterionic antifouling polymers, J. Phys. D Appl. Phys. 52 (40) (2019) 403001.
[24] H. Wang, Y. Wu, C. Cui, J. Yang, W. Liu, Antifouling super water absorbent supramolecular polymer hydrogel as an artificial vitreous body, Adv. Sci. 5 (11) (2018) 1800711.
[25] J.P. Mazzoccoli, D.L. Feke, H. Baskaran, P.N. Pintauro, Mechanical and cell viability properties of crosslinked low- and high-molecular weight poly(ethylene glycol) diacrylate blends, J. Biomed. Mater. Res. 93 (2) (2009) 558–566.
[26] R. Heidari, V. Ghanbarinejad, H. Mohammadi, A. Ahmadi, A. Esfandiari, N. Azarpira, H. Niknahad, Dithiothreitol supplementation mitigates hepatic and renal injury in bile duct ligated mice: potential application in the treatment of cholestasis-associated complications, Biomed. Pharmacother. 99 (2018) 1022–1032.
[27] J.P. Lopes De Almeida, C. Saldanha, Dithiothreitol revisited in red cells: a new head for an old hat, Clin. Hemorheol. Microcirc. 46 (1) (2010) 51–56.
[28] Z. Cao, N. Brault, H. Xue, A. Keefe, S. Jiang, Manipulating sticky and non-sticky properties in a single material, Angew. Chem. Int. Ed. 50 (27) (2011) 6102–6104.
[29] X. Dai, Y. Zhang, L. Gao, T. Bai, W. Wang, Y. Cui, W. Liu, A mechanically strong, highly stable, thermoplastic, and self-healable supramolecular polymer hydrogel, Adv. Mater. 27 (23) (2015) 3566–3571.
[30] G.L. Ellman, Tissue sulfhydryl groups, Arch. Biochem. Biophys. 82 (1) (1959) 70–77.
[31] T. Huang, H. Liu, P. Liu, P. Liu, L. Li, J. Shen, Zwitterionic copolymers bearing phosphonate or phosphonic motifs as novel metal-anchorable anti-fouling coatings, J. Mater. Chem. B 5 (27) (2017) 5380–5389.
[32] B.D. Mather, K. Viswanathan, K.M. Miller, T.E. Long, Michael addition reactions in macromolecular design for emerging technologies, Prog. Polym. Sci. 31 (5) (2006) 487–531.
[33] R. Razeghinejad, M.M. Lin, D. Lee, L.J. Katz, J.S. Myers, Pathophysiology and management of glaucoma and ocular hypertension related to trauma, Surv. Ophthalmol. 65 (5) (2020) 530–547.
[34] W.J. Foster, Vitreous substitutes, Expet Rev. Ophthalmol. 3 (2) (2014) 211–218.
[35] J. Chang, Y. Tao, B. Wang, X. Yang, H. Xu, Y. Jiang, B. Guo, Y. Huang, Evaluation of a redox-initiated in situ hydrogel as vitreous substitute, Polymer 55 (18) (2014) 4627–4633.
[36] J.H. de Groot, F.J. van Beijma, H.J. Haitjema, K.A. Dillingham, K.A. Hodd, S. A. Koopmans, S. Norrby, Injectable intraocular lens materials based upon hydrogels, Biomacromolecules 2 (3) (2001) 628–634.
[37] K. Wang, Z. Han, Injectable hydrogels for ophthalmic applications, J. Contr. Release 268 (2017) 212–224.
[38] J.R. Sparrow, K. Nakanishi, C.A. Parish, The lipofuscin fluorophore A2E mediates blue light-induced damage to retinal pigmented epithelial cells, Invest. Ophthalmol. Vis. Sci. 41 (7) (2000) 1981.
[39] Q. Liu, A. Chiu, L. Wang, D. An, W. Li, E.Y. Chen, L. Liu, Developing mechanically robust, triazole-zwitterionic hydrogels to mitigate foreign body response (FBR) for islet encapsulation, Biomaterials 230 (2020) 119640.
[40] A. Schulz, S. Wahl, A. Rickmann, J. Ludwig, B.V. Stanzel, H. von Briesen, P. Szurman, Age-related loss of human vitreal viscoelasticity, Transl. Vis. Sci. Techn. 8 (3) (2019) 56.
[41] M. Piccirelli, O. Bergamin, K. Landau, P. Boesiger, R. Luechinger, Vitreous deformation during eye movement, NMR Biomed. 25 (1) (2012) 59–66.
[42] P. Eiselt, K.Y. Lee, D.J. Mooney, Rigidity of two-component hydrogels prepared from alginate and poly(ethylene glycol)−diamines, Macromolecules 32 (17) (1999) 5561–5566.
[43] P.B. Welzel, S. Prokoph, A. Zieris, M. Grimmer, S. Zschoche, U. Freudenberg, C. Werner, Modulating biofunctional starPEG heparin hydrogels by varying size and ratio of the constituents, Polymers 3 (1) (2011) 602–620.
[44] J.A. Zimberlin, J.J. McManus, A.J. Crosby, Cavitation rheology of the vitreous: mechanical properties of biological tissue, Soft Matter 6 (15) (2010) 3632.
[45] K. Xue, Z. Liu, L. Jiang, D. Kai, Z. Li, X. Su, X.J. Loh, A new highly transparent injectable PHA-based thermogelling vitreous substitute, Biomater. Sci. 8 (3) (2019) 926–936.
[46] A.F. Silva, M.A. Alves, M.S.N. Oliveira, Rheological behaviour of vitreous humour, Rheol. Acta 56 (4) (2017) 377–386.
[47] S. Santhanam, Y.B. Shui, J. Struckhoff, B.B. Karakocak, P.D. Hamilton, G. J. Harocopos, N. Ravi, Bioinspired fibrillary hydrogel with controlled swelling behavior: applicability as an artificial vitreous, ACS Appl. Bio. Mater. 2 (1) (2019) 70–80.

[48] D.C. Murray, O.M. Durrani, P. Good, M.T. Benson, G.R. Kirkby, Biometry of the silicone oil-filled eye: II, Eye 16 (6) (1999) 319–324.
[49] N. Pasmanter, S.M. Petersen Jones, A review of electroretinography waveforms and models and their application in the dog, Vet. Ophthalmol. 23 (3) (2020) 418–435.
[50] X. Jiang, Y. Peng, C. Yang, W. Liu, B. Han, The feasibility study of an in situ marine polysaccharide-based hydrogel as the vitreous substitute, J. Biomed. Mater. Res. A. 106 (7) (2018) 1997–2006.